# Advantages Available in the Application of the Semi-Integral Electroanalysis Technique for the Determination of Diffusion Coefficients in the Highly Viscous Ionic Liquid 1-Methyl-3-Octylimidazolium Hexafluorophosphate

Cameron L. Bentley,[†,‡] Alan M. Bond,*[,†] Anthony F. Hollenkamp,[‡] Peter J. Mahon,[§] and Jie Zhang*[,†]

[†]School of Chemistry, Monash University, Clayton, Victoria 3800, Australia
[‡]CSIRO Energy Technology, Box 312, Clayton South, Victoria 3169, Australia
[§]Faculty of Life and Social Sciences, Swinburne University of Technology, Hawthorn, Victoria 3122, Australia

**S** *Supporting Information*

**ABSTRACT:** While it is common to determine diffusion coefficients from steady-state voltammetric limiting current values, derived from microelectrode/rotating disk electrode measurements or transient peak currents at macroelectrodes, application of these methods is problematic in highly viscous ionic liquids. This study shows that the semi-integral electroanalysis technique is highly advantageous under these circumstances, and it has allowed the diffusion coefficient of cobaltocenium, $[Co(Cp)_2]^+$ (simple redox process), and iodide, $I^-$ (complex redox mechanism), to be



*Semi-integration*

$$M(t) = \frac{d^{-1/2}I(t)}{dt^{-1/2}}$$

*I(t)* vs. *E*

$$M_L = nFAC^*\sqrt{D}$$

*M(t)* vs. *E*

determined in the highly viscous ionic liquid 1-methyl-3-octylimidazolium hexafluorophosphate (viscosity = 866 cP at 20 °C) from transient voltammograms obtained using a 1.6 mm diameter Pt electrode. In such a viscous medium, a near-steady-state current is not attainable with a 10 $\mu$m diameter microdisk electrode or a 3 mm diameter Pt rotating disk electrode, while peak currents at a macrodisk are subject to ohmic drop problems and the analysis is hampered by difficulties in modeling the processes involved in the oxidation of iodide. The diffusion coefficients of $[Co(Cp)_2]^+$ and $I^-$ were determined to be 9.4 ($\pm$0.3) $\times 10^{-9}$ cm² s⁻¹ and 7.3 ($\pm$0.3) $\times 10^{-9}$ cm² s⁻¹, respectively. These results highlight the utility of the semi-integral electroanalysis technique for quantifying the diffusivity of electroactive species in high viscosity media, where the use of steady-state techniques and transient peak currents is often limited.
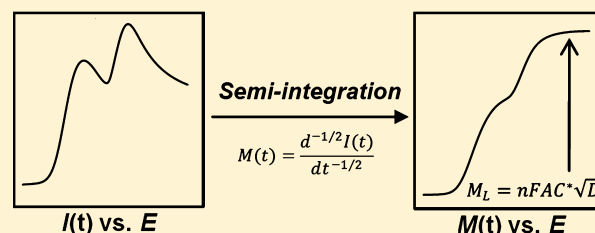
In recent years, there has been growing interest in replacing volatile molecular solvents with room temperature ionic liquids (RTILs) in a range of applications. Although the only truly ubiquitous property of RTILs is intrinsic ionic conductivity,[1] nonhaloaluminate ionic liquids often possess a number of attractive qualities, including negligible vapor pressure and high chemical, electrochemical, and thermal stability.[2] The physicochemical properties of a particular RTIL are determined by its constituent anion/cation and can therefore be tailored to suit specific applications.[3] One research area where RTILs have found application is in electrochemistry, where they have been successfully employed as alternative electrolytes in a range of electrochemical devices, including dye-sensitized solar cells, lithium batteries, and supercapacitors.[2,4,5]

The investigation and quantification of mass-transport (in the present case diffusivity) is of interest in any solvent, especially those employed in electrochemical devices, as it influences the ultimate rate/speed at which the device can operate. Potential sweep[6] or potential step[7] techniques are often employed to quantify the diffusivity of electroactive species in RTILs. In low viscosity molecular solvents, steady-state techniques, such as ultramicroelectrode (UME) voltammetry or rotating disk electrode (RDE) voltammetry, are generally advantageous over transient techniques as the measured steady-state mass transport limited currents are unaffected by sluggish electrode kinetics and/or high levels of uncompensated resistance. This allows the diffusion coefficient of the electroactive species to be determined using well-established theories.[8]

The viscosities of RTILs are typically 10−10 000 times higher than conventional molecular solvent (electrolyte) media. As a result, mass transport is significantly slower in RTILs, with diffusion coefficients often being in the range of $10^{-7}$ to $10^{-9}$ cm² s⁻¹ compared to $10^{-5}$ to $10^{-6}$ cm² s⁻¹ in molecular solvents. Consequently, in RTIL electrolytes, especially those with high viscosity, it is much more difficult to achieve a true steady state (at a disk UME), preventing the diffusion coefficient from being determined from the mass transport limited current.[9,10] It has also been shown that the RDE method suffers from similar problems,[10,11] arising from the difficulty in rotating the electrode at the sufficiently high rates

that are needed to achieve steady state under the highly viscous conditions.

In principle, diffusion coefficients can be calculated from the peak current of a dc linear sweep or cyclic voltammogram by employing the relationships described by the Randles–Sevcik equation for a reversible electron transfer process of the kind $Ox + ne^- \rightleftharpoons Red$ when the effect of uncompensated resistance is negligible.[8] In reality, very few of the electrochemical systems of interest in a viscous RTIL fulfill these criteria, limiting the direct application of dc voltammetry in the determination of diffusivity. Semi-integral electroanalysis is a technique pioneered by Oldham,[12−16] with semi-integration being specific for semi-infinite planar diffusion. It is related to the more general convolution procedure initially described by Savéant and co-workers[17] and later extended to other electrode geometries.[18] The technique involves semi-integrating the measured current with respect to time, giving rise to the function, $M(t)$, which is related to the concentration of the electroactive species at the electrode surface.

$$M(t) = \frac{d^{-1/2}I(t)}{dt^{-1/2}} \tag{1}$$

Semi-integrating a peak-shaped transient voltammogram ($I-E$) gives rise to a sigmoidal $M-E$ curve resembling a steady-state voltammogram.[8] As described in the theory of semi-integral electroanalysis, under purely diffusion controlled conditions (i.e., the concentration of analyte at the electrode surface is equal to zero), $M(t)$ reaches its limiting or maximum value, $M_L$:

$$M_L = nAFC^*\sqrt{D} \tag{2}$$

The diffusion coefficient, $D$, can therefore be determined from the $M_L$ plateau by transposing eq 2 if the stoichiometric number of electrons, $n$, active electrode area, $A$, and bulk concentration of electroactive species, $C^*$, are known along with the use of Faraday's constant, $F$.[8,13] The semi-integral electroanalysis technique shares a number of advantages with the previously discussed steady-state techniques without the need to record experimental data under steady-state conditions.

To demonstrate the advantage of using the semi-integral electroanalysis technique, this study aims to quantify diffusivity in a highly viscous RTIL, 1-methyl-3-octylimidazolium hexafluorophosphate, $[C_8mim][PF_6]$ ($\eta$ = 866 cP at 20 °C[19]), where the use of UME or RDE methods is impractical due to the difficulty in achieving a true steady state and $IR_u$ drop compromises peak current measurements with transient techniques at macrodisk electrodes. Two redox active species were the subject of investigations: cobaltocenium, $[Co(Cp)_2]^+$ ($Cp^- = C_5H_5^-$), which is known to undergo a mechanistically simple and electrochemically reversible one-electron reduction in RTILs[6] and iodide, $I^-$, which is known to undergo two oxidation processes with various degrees of reversibility in RTILs.[20−22]

## EXPERIMENTAL SECTION

**Reagents.** 1-Methyl-3-octylimidazolium hexafluorophosphate ($[C_8mim][PF_6]$, Solvent Innovation) was dried under high vacuum ($\leq 10^{-2}$ mbar) at 45 °C for 48 h and stored under lithium. The residual water was less than 25 ppm by Karl Fischer titration (Metrohm 831 KF Coulometer). 1-Ethyl-3-methylimidazolium iodide ($[C_2mim]I$, Io-li-tec GmbH, >98%) was recrystallized from a 2:1 mixture of ethyl acetate (Merck) and isopropanol (Merck) and then dried under high vacuum

for 48 h. Care was taken during handling and storage of $[C_2mim]I$ to avoid exposure to light. Cobaltocenium hexafluorophosphate ($[Co(Cp)_2][PF_6]$, Sigma-Aldrich) was used as supplied by the manufacturer. Acetonitrile was dried over activated alumina ($Al_2O_3$). Tetrabutylammonium hexafluorophosphate (TBAPF$_6$, Sigma) was dried under vacuum at 80 °C for 24 h. Ferrocene ($[Fe(Cp)_2]$, Fluka, >98%) and acetone (Merck) were used as supplied by the respective manufacturers. All of the above chemicals were stored and handled under a dry argon atmosphere in a glovebox.

**Electrochemical Systems and Procedures.** All voltammetric experiments were undertaken with a Gamry Reference 600 Potentiostat/Galvanostat/ZRA (Gamry Instruments, Warminster, PA). All experiments were carried out at ambient temperature (24 ± 1 °C). The solutions were degassed for at least 30 min with $N_2$ prior to experimentation and a blanket of $N_2$ was maintained over the electrolytes during the respective experiments. Microelectrode experiments were carried out inside a faraday cage using a 2-electrode arrangement with an Ag-wire quasi-reference electrode. Stationary macroelectrode and RDE experiments were carried out using a standard 3-electrode arrangement with a platinum flag auxiliary electrode and an Ag-wire or a Pt-wire quasi-reference electrode. All voltammetric measurements were carried out in at least triplicate. After performing the required voltammetric scans, the potential of the quasi-reference electrode was calibrated against the recommended $[Fe(Cp)_2]^{0/+}$ or $[Co(Cp)_2]^{+/0}$ process.[23,24]

The platinum macroelectrode (nominal diameter = 1.6 mm) and platinum UME (nominal diameter = 10 $\mu$m) were purchased from BASi (Bioanalytical systems, West Lafayette, IN) with the platinum rotating disk electrode (nominal diameter = 3.0 mm) purchased from Metrohm (Herisau, Switzerland). Prior to each new series of experiments, the pertinent electrodes were polished with aqueous 0.05 $\mu$m alumina slurry (Kemet Ltd., Kent, UK) on a clean polishing cloth (Buehler, Lake Bluff, IL). To remove adherent alumina, the electrodes were rinsed thoroughly with deionized water, rinsed with acetone, and allowed to dry at ambient temperature. Consistency of the electrode surfaces was checked using an optical microscope. The effective electrochemical area of the platinum macroelectrode was determined to be 0.0215 cm$^2$ by measuring the peak current obtained as a function of scan rate under linear sweep voltammetric conditions for the oxidation of $[Fe(Cp)_2]$ (2.0 mM in acetonitrile [0.1 M TBAPF$_6$]) and the use of the Randles−Sevcik equation [see eq 7]. The diffusion coefficient of $[Fe(Cp)_2]$ was taken to be $2.24 \times 10^{-5}$ cm$^2$ s$^{-1}$ under these conditions as published.[7]

Voltammetric simulations were undertaken using the DigiElch software (v. 4.0, Elchsoft, Germany). The algorithm used for semi-integration of the $I-t$ data was from de Levie,[25] which was adapted from Oldham and Myland.[26] A Microsoft Excel macro including this algorithm is available free online.[27] Experimental uncertainties were estimated by propagation of the standard deviations in the variables of interest.[28]

## RESULTS AND DISCUSSION

**$[Co(Cp)_2]^{+/0}$ Process.** The $[Co(Cp)_2]^{+/0}$ process has been characterized in a range of molecular solvents and RTILs and has been demonstrated to be a broadly useful reference scale by Bond and co-workers.[29] In some molecular solvents and RTILs, the $[Co(Cp)_2]^+$ cation has been shown to undergo two reversible one-electron reduction processes:

$$[Co(Cp)_2]^+ + e^- \rightleftharpoons [Co(Cp)_2]^0 \tag{3}$$

$$[Co(Cp)_2]^0 + e^- \rightleftharpoons [Co(Cp)_2]^- \tag{4}$$
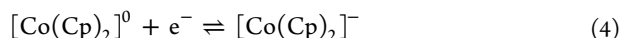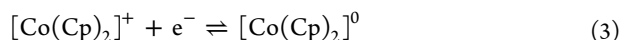
The second reduction process, $[Co(Cp)_2]^{0/-}$, is reportedly solvent dependent,[23] and for this reason, only the first process was the subject of investigations in this study.

*Ultramicroelectrode Studies.* In principle, the diffusion coefficient $(D)$ of an electroactive species can be calculated from the steady-state limiting current $(I_L)$ measured at a disk UME using the expression:[8]

$$I_L = 4nFC^*aD \tag{5}$$

where $a$ is the radius of the electrode. A cyclic voltammogram obtained from 9.96 mM $[Co(Cp)_2][PF_6]$ in $[C_8mim][PF_6]$ at a 10 $\mu$m diameter Pt UME is shown in Figure 1. The waveshape
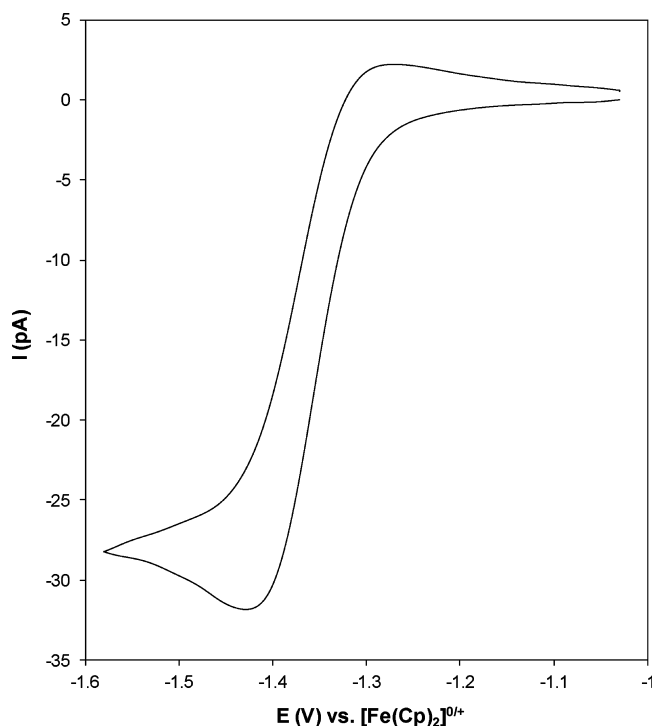


**Figure 1.** Cyclic voltammogram obtained from 9.96 mM $[Co(Cp)_2]$-$[PF_6]$ in $[C_8mim][PF_6]$ at a 5 $\mu$m radius Pt UME with a scan rate of 5 mV s$^{-1}$.

in this RTIL is intermediate between a sigmoidal and a peak-shaped voltammogram, implying that radial diffusion contributes significantly to mass transport. Despite the small electrode size $(a = 5\ \mu m)$ and slow voltammetric scan rate $(5\ \text{mV s}^{-1})$, even near steady-state conditions have not been attained and for this reason calculating the diffusion coefficient using eq 5 is not possible. Attempting to extract a "limiting current" from a voltammogram obtained under these mixed transient/steady-state conditions leads to an overestimate of the true steady-state limiting current.[30] The true steady-state current could be predicted using a procedure known as convolutive forecasting; however, in order to apply the convolving function, it is necessary to know the values of $D$ and $a$, whereas semi-integration only requires the current.[31] Alternatively, the diffusion coefficient could be estimated from this mixed transient/steady-state voltammogram using a "best-fit" approach via numerical simulation with DigiElch.

In principle, in order to approach a true steady state, either a much smaller electrode or a slower scan rate can be employed. However, these approaches are generally impractical due to the high viscosity of RTILs which can result in a diffusion coefficient of the order of $10^{-9}\ \text{cm}^2\ \text{s}^{-1}$. Under these conditions, an impractically small electrode (difficulty in both electrode fabrication and current measurement) or slow scan rate would have to be used for true steady-state measurements (see detailed discussion in the Supporting Information section).

*Rotating Disk Electrode Studies.* In theory, the diffusion coefficient of an electroactive species can also be calculated from the steady-state limiting current measured at the RDE using the Levich equation:[26]

$$I_L = 0.620nFA\left(\frac{d}{\eta}\right)^{1/6} D^{2/3}\omega^{1/2}C^* \tag{6}$$

where $d$ is the density of the electrolyte, $\eta$ is the dynamic viscosity of the electrolyte, and $\omega$ is the angular rotation rate of the electrode. Cyclic voltammograms obtained from 10.1 mM $[Co(Cp)_2][PF_6]$ in $[C_8mim][PF_6]$ at a 3.0 mm diameter Pt RDE are shown in Figure 2. The waveshape in this RTIL at 500
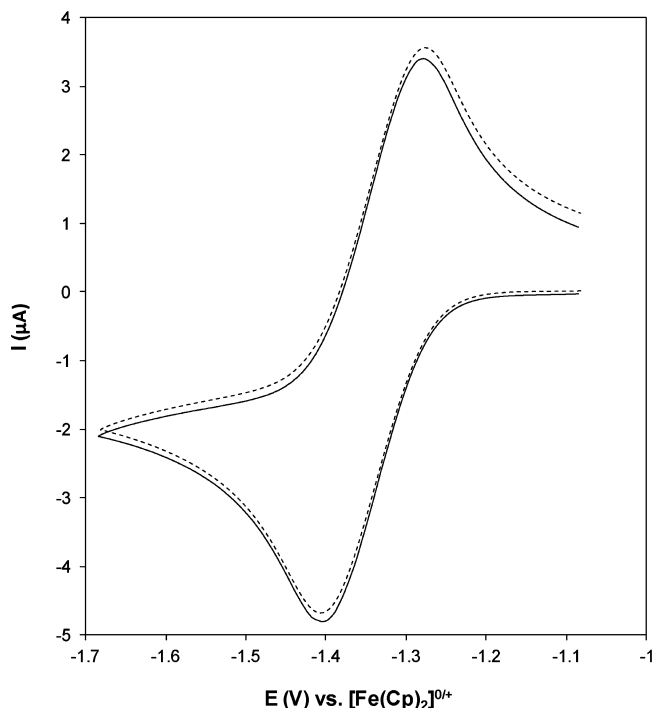


**Figure 2.** Cyclic voltammograms obtained from 10.1 mM $[Co(Cp)_2]$-$[PF_6]$ in $[C_8mim][PF_6]$ at a 1.5 mm radius Pt RDE with a scan rate of 50 mV s$^{-1}$ and rotation speeds of 0 rpm (dashed trace) and 500 rpm (solid trace).

rpm is almost identical to when the electrode is stationary (0 rpm) implying that mass transport is governed predominantly by planar diffusion at this rotation speed, accentuating the fact that forced convection is relatively ineffective in high viscosity fluids. Once again, because steady-state conditions have not been attained, the diffusion coefficient cannot be calculated using eq 6 and would have to be estimated using a "best-fit" approach with numerical simulation.

In principle, in order to approach a true steady state, much higher rotation speeds could be employed. In practice, however, this approach is not feasible, as it was found that air bubbles

become trapped at the electrode−electrolyte interface at high rotation speeds (>500 rpm), giving rise to noisy and irreproducible current data (see Figure S2, Supporting Information). Similar problems were encountered by Zhao et al.[11] when performing RDE experiments in a range of high viscosity room temperature protic ionic liquids (RTPILs). Simulations revealed that rotation speeds in excess of 5000 rpm would be required to approach a true steady state in RTPILs with viscosities that are lower than that of $[C_8mim][PF_6]$.

*Macrodisc Electrode Studies.* In light of the practical difficulties in approaching true steady-state conditions in $[C_8mim][PF_6]$, transient voltammetric techniques were applied in order to quantify the diffusivity of $[Co(Cp)_2]^+$ in this RTIL. Since $[Co(Cp)_2]^{+/0}$ is a well-known reversible process, $D$ can be calculated from the transient peak current ($I_p$) using the Randles−Sevcik equation when the $IR_u$ effect is negligible:[8]

$$I_p = 0.4463nFA\left(\frac{nFD\nu}{RT}\right)^{1/2}C^* \tag{7}$$

where $R$ is universal gas constant, $\nu$ is the voltammetric scan rate, and $T$ is the temperature.

Cyclic voltammograms obtained from 9.96 mM $[Co(Cp)_2]$-$[PF_6]$ in $[C_8mim][PF_6]$ at multiple scan rates at a Pt macroelectrode are shown in Figure 3a. As expected, a chemically reversible reduction process corresponding to eq 3 was observed at all of the investigated scan rates. Peak separations ($\Delta E_p$) were larger than the expected 56.8 mV for a reversible process at 24 °C and increased significantly with increasing scan rate with values of 67, 83, and 100 mV at 10, 25, and 50 mV s$^{-1}$, respectively. Given that it has been demonstrated that the $[Co(Cp)_2]^{+/0}$ process displays ideal electrochemical reversibility in a range of molecular solvents[23] and RTILs,[6,32] the large $\Delta E_p$ values are likely due to the effect of uncompensated resistance ($IR_u$). On the basis of the geometry of the electrode ($a$ = 0.8 cm) and the ionic conductivity ($\kappa$) of $[C_8mim][PF_6]$, 0.26 mS cm$^{-1}$ at 25 °C,[33] uncompensated resistance is estimated ($R_u \approx 1/4\kappa r$)[34] to be ~12 kΩ, which accounts for the significant distortion seen in the voltammograms shown in Figure 3a.

The peak current is predicted to be proportional to the square root of scan rate, which was not the case for the data shown in Figure 3a, evidenced by the nonzero intercept of the linear plot shown in Figure 3b. Nevertheless, the diffusion coefficient of $[Co(Cp)_2]^+$ was determined to be 7.6 ($\pm$0.2) $\times$ 10$^{-9}$ cm$^2$ s$^{-1}$ from the slope of the $I_p$ vs $\nu^{1/2}$ curve, obtained by linear regression of the experimental data, by substituting the appropriate values of known parameters into eq 7. As expected, the calculated diffusion coefficient of $[Co(Cp)_2]^+$ in $[C_8mim]$-$[PF_6]$ is orders of magnitude lower than that reported in acetonitrile, 1.64 $\times$ 10$^{-5}$ cm$^2$ s$^{-1}$ at 23 °C[32] and $[C_2mim]$-$[NTf_2]$, 3.27 $\times$ 10$^{-7}$ cm$^2$ s$^{-1}$ at 23 °C[6] in accordance with the relative viscosities of the respective solvents. However, it should be noted that, due to the presence of significant $IR_u$ effect, the diffusion coefficient obtained on the basis of peak current and application of eq 7 is expected to be smaller than the true value with the presence of uncompensated resistance resulting in a nonzero intercept in Figure 3b. Forcing the linear line of best fit through the origin lowers the coefficient of determination ($R^2$ = 0.9968) and changes the slope of the $I_p$ vs $\nu^{1/2}$ curve, demonstrating that this approach is unsuitable under the circumstances. In order to obtain a more accurate $D$ value, numerical simulations that accommodate the contribution from
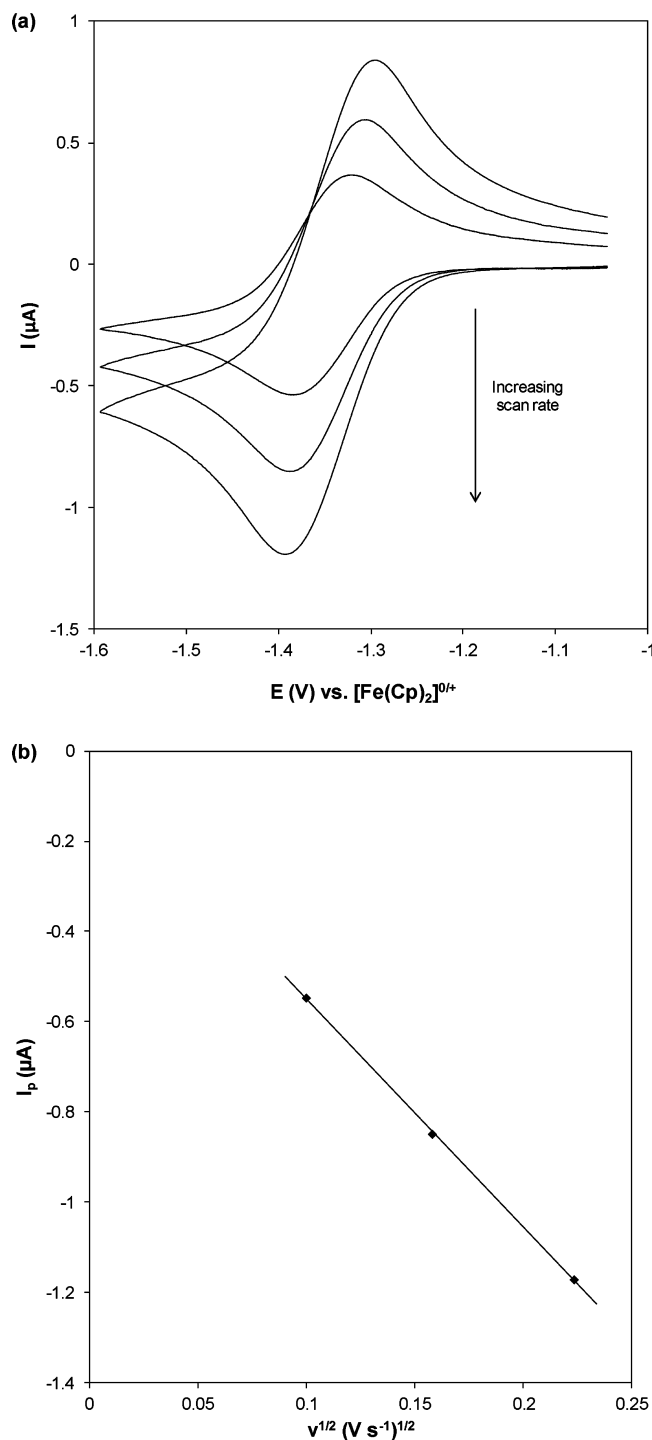


**Figure 3.** (a) Cyclic voltammograms obtained from 9.96 mM $[Co(Cp)_2][PF_6]$ in $[C_8mim][PF_6]$ at a 0.8 mm radius Pt macroelectrode with scan rates (from top to bottom) of 50, 25, and 10 mV s$^{-1}$. (b) Linear plot of mean peak current (from triplicate experiments) vs the square root of the scan rate ($R^2$ = 0.9998).

$R_u$ were undertaken and a $D$ value of 9.0 ($\pm$0.2) $\times$ 10$^{-9}$ cm$^2$ s$^{-1}$ was obtained from simulation/experiment comparison (see Figure S3, Supporting Information). This is significantly greater than the value obtained from the direct use of the peak currents and demonstrates the effect of uncompensated resistance when using peak currents to estimate the diffusion coefficient.

*Semi-integral Analysis Studies.* The semi-integral electroanalysis technique is unaffected by sluggish electrode kinetics or

$IR_u$ and does not require comparison with a simulation, making it preferable to the Randles–Sevcik method. $M$–$E$ curves before and after background subtraction for the $[Co(Cp)_2]^{+/0}$ process are shown in Figure 4. As can be seen in this figure,
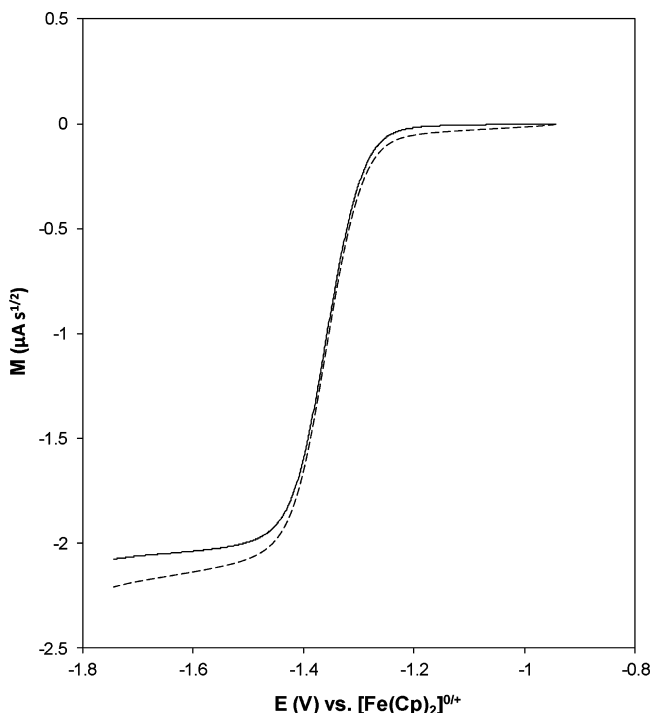


**Figure 4.** $M$–$E$ curves obtained from 9.96 mM $[Co(Cp)_2][PF_6]$ in $[C_8mim][PF_6]$ at a 0.8 mm radius Pt macroelectrode with a scan rate of 50 mV s$^{-1}$ before (dashed curve) and after (solid curve) background subtraction.

there is a significant slope in the $M_L$ plateau prior to background subtraction, which can be attributed to charging of the electrical double layer at the stationary electrode. At the analyte concentration used, the contribution from double layer charging current to the total current can be significant. If the double layer capacitance is potential independent, the $M_C$–$E$ ($M_C$ = semi-integration of capacitance current) curve will not be potential independent as the semi-integration of a constant introduces a $t^{1/2}$ dependence. This becomes more complicated when the capacitance is potential dependent.[13] Therefore, the background current was measured in the absence of $[Co(Cp)_2]^+$ and subtracted from the total current. The diffusion coefficient of $[Co(Cp)_2]^+$ was then determined to be 9.4 ($\pm$0.3) $\times$ 10$^{-9}$ cm$^2$ s$^{-1}$ using the $M_L$ value taken at −1.55 V vs $[Fe(Cp)_2]^{0/+}$ and by substituting the appropriate values into eq 2. This $D$ value is in good agreement with that of 9.0 ($\pm$0.2) $\times$ 10$^{-9}$ cm$^2$ s$^{-1}$ obtained using transient cyclic voltammetry with numerical simulation.

**$I^-/I_3^-/I_2$ Processes. *Semi-integral Analysis Studies.*** Analogous to its behavior in aprotic solvents such as acetonitrile,[35,36] iodide has been shown to undergo two oxidation processes in a range of RTILs to produce molecular iodine as per eqs 8 and 9:[8,14,24]

$$3I^- \rightleftharpoons I_3^- + 2e^- \tag{8}$$

$$I_3^- \rightleftharpoons \frac{3}{2}I_2 + e^- \tag{9}$$

The reaction mechanism is complicated by the following homogeneous equilibrium process:

$$I^- + I_2 \rightleftharpoons I_3^- \tag{10}$$

Overall, it is a one-electron per iodine atom process with much greater mechanistic complexity than the previously investigated $[Co(Cp)_2]^{+/0}$ process.

Cyclic voltammograms obtained from 14.3 mM $[C_2mim]I$ in $[C_8mim][PF_6]$ at multiple scan rates at a Pt macroelectrode are shown in Figure 5. At all of the investigated scan rates, there are
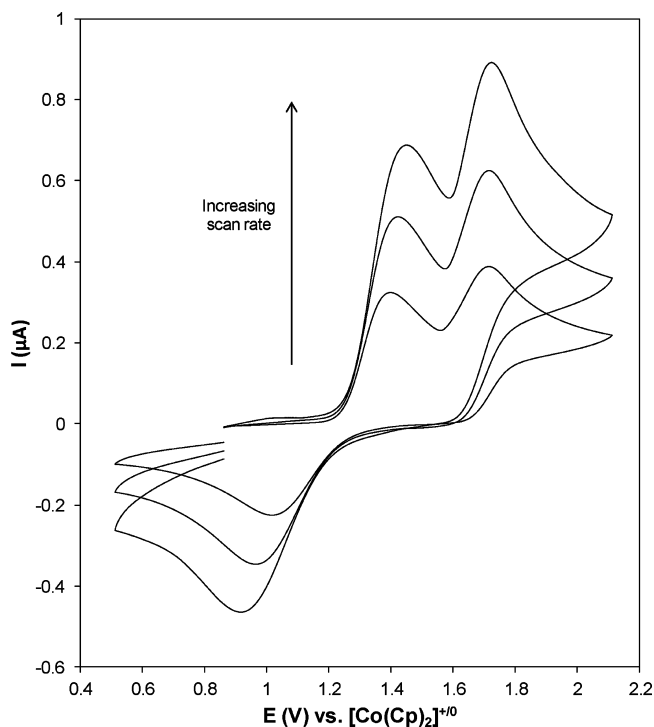


**Figure 5.** Cyclic voltammograms obtained from 14.3 mM $[C_2mim]I$ in $[C_8mim][PF_6]$ at a 0.8 mm radius Pt macroelectrode with scan rates (from top to bottom) of 50, 25, and 10 mV s$^{-1}$.

two peaks on the forward sweep, corresponding to the $I^-/I_3^-$ and $I_3^-/I_2$ processes shown in eqs 8 and 9, respectively. On the reverse sweep, the reduction peak for the $I_2/I_3^-$ process, eq 9, is not well-defined, and the reduction peak associated with the $I_3^-/I^-$ process, eq 8, is asymmetric with respect to the oxidation peak, with large $\Delta E_p$ values of 383, 460, and 536 mV at 10, 25, and 50 mV s$^{-1}$, respectively. Indeed, the first oxidation process has been reported to be kinetically sluggish and electrochemically irreversible in a range of imidazolium RTILs.[20−22]

The mechanistic complexity and sluggish heterogeneous kinetics of the iodide oxidation process precludes the direct application of the relationship described by the Randles–Sevcik equation and the use of numerical simulation to quantify diffusivity. Consequently, the semi-integral electroanalysis technique was applied; $M$–$E$ curves before and after background subtraction obtained from 14.3 mM $[C_2mim]I$ in $[C_8mim][PF_6]$ are shown in Figure 6. There are two plateaus on the $M$–$E$ curve corresponding to the $I^-/I_3^-$ and $I_3^-/I_2$ processes shown in eqs 8 and 9, respectively. The size of the plateaus relative to each other are expected to be proportional to the number of electrons involved in each redox process (2:1); however, it is difficult to accurately measure the magnitude of the first plateau due to overlap caused by the
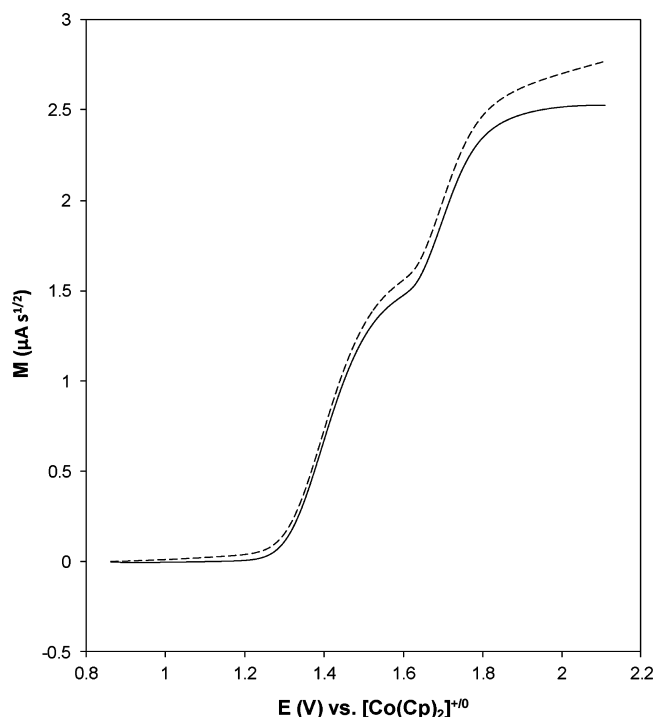
**Figure 6.** $M-E$ curves obtained from 14.3 mM $[C_2mim]I$ in $[C_8mim][PF_6]$ at a 0.8 mm radius Pt macroelectrode with a scan rate of 50 mV s$^{-1}$ before (dashed curve) and after (solid curve) background subtraction.

closeness of half-wave potentials, resulting in the observation of a ~3:2 ratio. Attempting to extract a $M_L$ value from such a poorly defined "plateau" would inevitably lead to an inaccurate determination of $D$. Once again, there is quite a significant slope in the $M_L$ plateau prior to background subtraction, which was corrected for in the same way as previously described. The diffusion coefficient of I$^-$ was determined to be 7.3 ($\pm$0.3) $\times$ $10^{-9}$ cm$^2$ s$^{-1}$ using the $M_L$ value taken at 2.0 V vs $[Co(Cp)_2]^{+/0}$ and by substituting the appropriate values into eq 2. Unsurprisingly, the calculated diffusion coefficient of I$^-$ in $[C_8mim][PF_6]$ is orders of magnitude lower than that reported in acetonitrile, 1.68 $\times$ $10^{-5}$ cm$^2$ s$^{-1}$ at 25 °C,[36] and $[C_2mim][NTf_2]$, 2.68 $\times$ $10^{-7}$ cm$^2$ s$^{-1}$ at 25 °C[37] in accordance with the relative viscosities of the respective electrolytes.

Microelectrode measurements in this system again do not approach the near-steady-state condition, and RDE methods cannot be used for the reasons noted above. The determination of the diffusion coefficients of both $[Co(Cp)_2]^+$ and I$^-$ using transient techniques without resorting to numerical simulation is therefore highly advantageous.

## CONCLUSIONS

The relative merits of several voltammetric methods have been evaluated for the purposes of determining the diffusion coefficient of cobaltocenium and iodide in the high viscosity room temperature ionic liquid 1-methyl-3-octylimidazolium hexafluorophosphate. It was found that the viscosity of the electrolyte was too high to practicably approach true steady-state conditions over a reasonable experimental time scale, ruling out the use of steady-state UME theory to quantify diffusivity. Similarly, the steady-state RDE theory was unable to be applied due to the difficulties associated with rotating the electrode at sufficient rates in the high viscosity electrolyte. The

diffusion coefficient of cobaltocenium measured using transient voltammetry and the Randles−Sevcik method was significantly underestimated due to the effect of uncompensated resistance. Therefore, a reliable $D$ value under these circumstances requires comparison of the experimental cyclic voltammogram with a simulated one. In contrast, the semi-integral electroanalysis method does not suffer from the effect of uncompensated resistance, allowing the $D$ value to be determined efficiently with high accuracy, with the use of a simple equation. The advantages of using the semi-integral electroanalysis method are even more important when used for the successful determination of the $D$ value of I$^-$ in a I$^-$/I$_3^-$/I$_2$ model system, where the application of the Randles−Sevcik method is invalid and numerical simulations are problematic due to the mechanistic complexity and kinetic sluggishness of the iodide oxidation process.

## ASSOCIATED CONTENT

**Supporting Information**
Further discussion on the applicability of steady-state techniques in RTILs (Figure S1), demonstration of the practical difficulties in rotating the RDE at high rates in viscous media (Figure S2), and numerical simulations of the $[Co(Cp)_2]^{+/0}$ process (Figure S3). This material is available free of charge via the Internet at http://pubs.acs.org

## AUTHOR INFORMATION

**Corresponding Author**
*E-mail: alan.bond@monash.edu (A.M.B.); jie.zhang@monash.edu (J.Z.).
**Notes**
The authors declare no competing financial interest.

## REFERENCES

(1) MacFarlane, D. R.; Seddon, K. R. *Aust. J. Chem.* **2007**, *60*, 3−5.
(2) Armand, M.; Endres, F.; MacFarlane, D. R.; Ohno, H.; Scrosati, B. *Nat. Mater.* **2009**, *8*, 621−629.
(3) Dean, P. M.; Pringle, J. M.; MacFarlane, D. R. *Phys. Chem. Chem. Phys.* **2010**, *12*, 9144−9153.
(4) Galinski, M.; Lewandowski, A.; Stepniak, I. *Electrochim. Acta* **2006**, *51*, 5567−5580.
(5) Fernicola, A.; Scrosati, B.; Ohno, H. *Ionics* **2006**, *12*, 95−102.
(6) Sukardi, S. K.; Zhang, J.; Burgar, I.; Horne, M. D.; Hollenkamp, A. F.; MacFarlane, D. R.; Bond, A. M. *Electrochem. Commun.* **2008**, *10*, 250−254.
(7) Rogers, E. I.; Silvester, D. S.; Poole, D. L.; Aldous, L.; Hardacre, C.; Compton, R. G. *J. Phys. Chem. C* **2008**, *112*, 2729−2735.
(8) Bard, A. J.; Faulkner, L. R. *Electrochemical methods: fundamentals and applications*, 2nd ed.; Wiley: New York, 2001.
(9) Zhang, J.; Bond, A. M. *Analyst* **2005**, *130*, 1132−1147.
(10) Barrosse-Antle, L. E.; Bond, A. M.; Compton, R. G.; O'Mahony, A. M.; Rogers, E. I.; Silvester, D. S. *Chem.-Asian J.* **2010**, *5*, 202−230.
(11) Zhao, C.; Burrell, G.; Torriero, A. A. J.; Separovic, F.; Dunlop, N. F.; MacFarlane, D. R.; Bond, A. M. *J. Phys. Chem. B* **2008**, *112*, 6923−6936.
(12) Grenness, M.; Oldham, K. B. *Anal. Chem.* **1972**, *44*, 1121−1129.
(13) Oldham, K. B. *Anal. Chem.* **1972**, *44*, 196−198.
(14) Goto, M.; Oldham, K. B. *Anal. Chem.* **1973**, *45*, 2043−2050.
(15) Goto, M.; Oldham, K. B. *Anal. Chem.* **1974**, *46*, 1522−1530.
(16) Oldham, K. B. *J. Electroanal. Chem.* **1976**, *72*, 371−378.
(17) Saveant, J. M. *J. Electroanal. Chem.* **1973**, *44*, 169−187.

(18) Mahon, P. J.; Oldham, K. B. *J. Electroanal. Chem.* **1999**, *464*, 1–13.

(19) Seddon, K. R.; Stark, A.; Torres, M. J. Viscosity and density of 1-alkyl-3-methylimidazolium ionic liquids. In *Clean Solvents: Alternative Media for Chemical Reactions and Processing*; Abraham, M. A., Moens, L., Eds.; American Chemical Society: Washington, DC, 2002; Vol. *819*, p 34–49.

(20) Zhang, Y.; Zheng, J. B. *Electrochim. Acta* **2007**, *52*, 4082–4086.

(21) Ejigu, A.; Lovelock, K. R. J.; Licence, P.; Walsh, D. A. *Electrochim. Acta* **2011**, *56*, 10313–10320.

(22) Silvester, D. S.; Aldous, L.; Hardacre, C.; Compton, R. G. *J. Phys. Chem. C* **2008**, *112*, 6551–6557.

(23) Stojanovic, R. S.; Bond, A. M. *Anal. Chem.* **1993**, *65*, 56–64.

(24) Gritzner, G.; Kuta, J. *Pure Appl. Chem.* **1984**, *56*, 461–466.

(25) de Levie, R. *How to Use Excel® in Analytical Chemistry and in General Scientific Data Analysis*; Cambridge University Press: Cambridge, 2001.

(26) Oldham, K. B.; Myland, J. C. *Fundamentals of electrochemical science*; Academic Press: San Diego, 1994.

(27) de Levie, R. Excellaneous. http://www.bowdoin.edu/~rdelevie/excellaneous/ (accessed June 18, 2012).

(28) Skoog, D. A.; West, D. M.; Holler, F. J.; Crouch, S. R. *Fundamentals of analytical chemistry*, 8th ed.; Thomson-Brooks/Cole: Belmont, CA, 2004.

(29) Hultgren, V. M.; Mariotti, A. W. A.; Bond, A. M.; Wedd, A. G. *Anal. Chem.* **2002**, *74*, 3151–3156.

(30) Buzzeo, M. C.; Evans, R. G.; Compton, R. G. *ChemPhysChem* **2004**, *5*, 1106–1120.

(31) Mahon, P. J. *J. Solid State Electrochem.* **2009**, *13*, 573–582.

(32) Shiddiky, M. J. A.; Torriero, A. A. J.; Zhao, C.; Burgar, I.; Kennedy, G.; Bond, A. M. *J. Am. Chem. Soc.* **2009**, *131*, 7976–7989.

(33) Kanakubo, M.; Harris, K. R.; Tsuchihashi, N.; Ibuki, K.; Ueno, M. *Fluid Phase Equilib.* **2007**, *261*, 414–420.

(34) Creager, S. Solvents and Supporting Electrolytes. In *Handbook of Electrochemistry*; Zoski, C. G., Ed.; Elsevier: Amsterdam, 2007; Chapter 3, p 57–72.

(35) Hanson, K. J.; Tobias, C. W. *J. Electrochem. Soc.* **1987**, *134*, 2204–2210.

(36) Macagno, V. A.; Giordano, M. C.; Arvia, A. J. *Electrochim. Acta* **1969**, *14*, 335.

(37) Kawano, R.; Watanabe, M. *Chem. Commun.* **2003**, 330–331.